ChemComm

COMMUNICATION

View Article Online
View Journal | View Issue

Cite this: *Chem. Commun.*, 2023, 59, 11129

Received 21st July 2023,
Accepted 23rd August 2023

DOI: 10.1039/d3cc03508e

rsc.li/chemcomm

Synthesis of penta- and hexa(3,4-thienylene): size-dependent structural properties of cyclic oligothiophenes†

Mai Nagase, [ab] Sachiko Nakano[a] and Yasutomo Segawa *[ab]

Penta- and hexa(3,4-thienylene)s were synthesized as a potential precursor for thiophene-containing polyarenes, and the structures were determined *via* X-ray crystallography. The interconversion of thiophene rings is fast in penta(3,4-thienylene), and slow in hexa(3,4-thienylene) reflecting the activation energy for enantiomerization. Size-dependent bathochromic shifts were observed in UV-vis absorption spectra.

Cyclic oligoarylenes have long received considerable attention due to their structural, electronic, and optical properties.[1] The most representative arylenes are phenylenes, in which the phenyl groups can be connected to each other in three ways, *i.e.*, at the *o*-, *m*-, or *p*-positions. Of these, cyclo-*o*-phenylenes are of little interest and are not very well explored. Even so, biphenylene, triphenylene, tetraphenylene, hexaphenylene, and octaphenylene derivatives have already been synthesized (Fig. 1a), and their reactivity, structural properties, and applications have been investigated.[2] Replacing the benzene rings with thiophene rings allows modifying the electronic and structural properties to induce, for example, weaker aromaticity, lower steric hindrance, and intermolecular S···S interactions in the solid state.[3] Structurally, cyclo-*o*-phenylenes correspond approximately to cyclic oligo(3,4-thienylene)s in as much that the thiophene rings are linked at the β,β′-positions (Fig. 1b). To date, cyclic oligo(3,4-thienylene)s with two to four thiophene rings[4] have been explored. Given that all their α-positions are reactive sites, tri- and tetra(3,4-thienylene)s (**3T** and **4T**) can be transformed into a variety of electron-rich π-conjugated molecules, such as heterosumanenes[5] and hetero[8]circulenes,[6] as well as tetra(3,4-thienylene)s can be employed as *e.g.*, 3D building blocks[7] or solvent-responsive molecular assemblies.[8] In addition, tri(3,4-thienylene)s have been studied as charge-transfer complexes[9] or planar [6]radialenes.[10] However, cyclic oligo(3,4-thienylene)s with five or more thiophene rings have not yet been synthesized.[11] To create larger β,β′-linked cyclic oligo(3,4-thienylene)s, building blocks that contain functional groups at the β-positions are a prerequisite. In 2017, a practical synthetic method for a β-substituted unit, *i.e.*, a 3,4-diborylated thiophene derivative, was developed by Osuka, Tanaka, and co-workers, which widened the range of synthetic approaches for cyclic compounds that contain 3,4-thienylenes and other heteroarenes.[12]

Herein, we report the synthesis of penta- and hexa(3,4-thienylene)s (**5T** and **6T**) *via* Pd-catalyzed cross-coupling and Ni-mediated homocoupling reactions using 3,4-diborylthiophene **1** or the newly synthesized 4,4′-diboryl-3,3′-bithiophene **2** (Fig. 1c and 2a). The structures and electronic properties of **5T** and **6T** were determined using NMR and X-ray crystallography as well as UV-vis absorption spectroscopy. The structural characteristics and optoelectronic properties of **5T** and **6T** were compared to

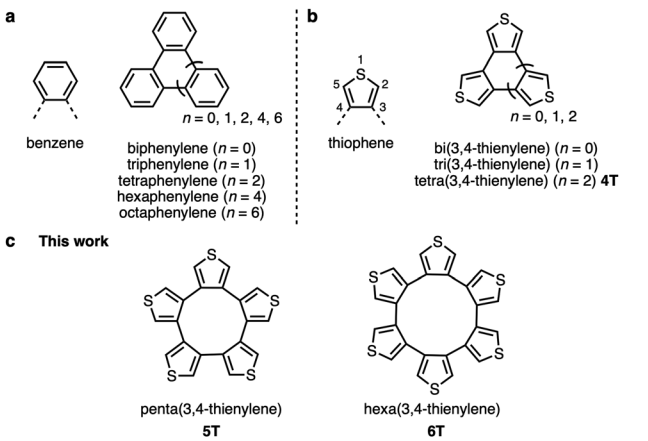

Fig. 1 Representative cyclic oligoarylenes. (a) Cyclo-*o*-phenylenes. (b) Cyclic oligo(3,4-thienylene)s. (c) Penta- and hexa(3,4-thienylene)s (**5T** and **6T**).

[a] *Institute for Molecular Science, Myodaiji, Okazaki, 444-8787, Japan. E-mail: segawa@ims.ac.jp*

[b] *The Graduate University for Advanced Studies, SOKENDAI, Myodaiji, Okazaki, 444-8787, Japan*

† Electronic supplementary information (ESI) available: CCDC 2281496 (**2**), 2281497 (**5T**) and 2281498 (**6T**). For ESI and crystallographic data in CIF or other electronic format see DOI: https://doi.org/10.1039/d3cc03508e

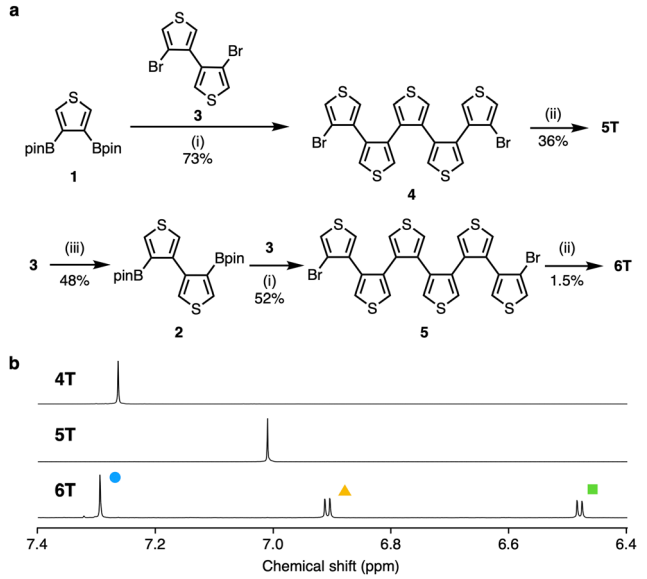

Fig. 2 (a) Synthesis of **5T** and **6T**; (i) $Pd_2(dba)_3$, XPhos, K_3PO_4, THF/H_2O, 40 °C, 22–23 h; (ii) Ni(cod)$_2$, 2,2′-bipyridine, THF, reflux, 2.5 h; (iii) HBpin, Zn powder, Et_3N, $NiCl_2$(dppp), DPPF, toluene, reflux, 60 h. (b) ^{1}H NMR spectra of **4T**–**6T** in CD_2Cl_2. The signals of **6T** are indicated by colored marks. Abbreviations: dba = dibenzylideneacetone; XPhos = 2-dicyclohexylphosphino-2′,4′,6′-triisopropylbiphenyl; cod = 1,5-cyclooctadiene; Bpin = 4,4,5,5-tetramethyl-1,3,2-dioxaborolan-2-yl; dppp = 1,3-bis(diphenylphosphino)propane; DPPF = 1,1′-bis(diphenylphosphino)ferrocene.

those of **4T**, and examined using density functional theory (DFT) calculations.

Penta- and hexa(3,4-thienylene)s (**5T** and **6T**) were synthesized *via* sequential Suzuki–Miyaura cross-coupling and Ni(0)-mediated intramolecular homocoupling reactions (Fig. 2a). For that purpose, diborylthiophene **1** and 4,4′-dibromo-3,3′-bithiophene (**3**) were prepared initially according to reported methods.[12,13] The Suzuki–Miyaura cross-coupling reaction of **1** with an excess of **3** (8.0 equiv.) was carried out using $Pd_2(dba)_3$ (2.5 mol%), XPhos (10 mol%), and K_3PO_4 (4.0 equiv.) to produce dibromoquinquethiophene **4** in 73% yield. Dibromobithiophene **3** was used in excess in order to suppress the generation of polymers. The resulting **4** was treated with Ni(cod)$_2$ (2.2 equiv.) and 2,2′-bipyridine (2.2 equiv.) for 3 h in refluxing tetrahydrofuran (THF) (2 mM), which allowed isolating the desired cyclic oligothiophene **5T** in 36% yield. Increasing the substrate concentration provided **5T** in low yield in this reaction step. Next, a cyclic oligothiophene containing an additional thiophene ring, **6T**, was synthesized by applying analogous reaction conditions. A borylation reaction similar to that used to synthesize **1**[12,14] was performed to obtain **2** in 48% yield. The reaction of **2** with an excess of **3** under Pd catalysis furnished dibromosexithiophene **5** in 52% yield. The obtained **5** was subsequently treated with Ni(cod)$_2$ (3.3 equiv.) and 2,2-bipyridine (3.3 equiv.) in THF. In contrast to **5T**, **6T** was obtained in low yield (1.5%), presumably due to the formation of polymeric compounds. Both **5T** and **6T** were slightly soluble in common organic solvents (see Table S1 in ESI† for details).

To identify the thus-obtained compounds **5T** and **6T**, and to investigate their size-dependent structural characteristics, NMR spectra were recorded (Fig. 2b). In the room-temperature ^{1}H NMR spectrum of **5T** in dichloromethane-d_2, the α-protons of the thiophene rings appear as a singlet at 7.01 ppm. Even at −95 °C, the singlet remains almost unchanged. In the ^{13}C NMR spectrum in chloroform-d_1, two signals were observed at 124.6 and 137.6 ppm. These results indicate that the dynamic interconversion of the thiophene rings is fast on the NMR timescale. Unlike that of **5T**, the ^{1}H NMR spectrum of **6T** in dichloromethane-d_2 at room temperature displays three signals, *i.e.*, doublets at 6.5 and 6.9 ppm as well as a singlet at 7.3 ppm. Only very slight broadening of the signals was observed even at 140 °C in tetrachloroethane-d_2, indicating that **6T** has three diastereotopic protons and those are not exchanged in the NMR timescale. The ^{1}H NMR spectra of **4T**–**6T** presented in Fig. 2b clearly demonstrate the size dependence of the symmetry in solution. The NMR assignments were supported by chemical shift calculations using the GIAO method (see Fig. S2 in ESI† for details).

The solid-state structures of **5T** and **6T** were determined *via* X-ray diffraction analysis of single crystals obtained from a hexane/chloroform and a pentane/THF solution, respectively (Fig. 3a and b). Compound **5T** adopts a C_2-symmetric structure in which five thiophene rings are fused at the 3,4-positions to form a 10-membered ring. Compound **6T** adopts a screw (or helical) structure with D_2 symmetry, similar to hexaphenylene[2b,e–h] and hexa(2,3-thienylene)s.[11b,f] The distance between the centroids of the central thiophene rings (av. 3.4 Å) is typical for intramolecular π–π interactions. In both crystals, the enantiomers are aligned alternatingly reflecting the centric space group (*I*2/*a*). The average dihedral angles (θ) of the α–β–β–α and β–β–β–β positions of the 3,3′-bithiophene moieties are shown in Fig. 3a and b. The dihedral angles in **5T** and **6T** are 46.0° (θ_a), 90.8° (θ_b), and 87.8° (θ_c), and 41.8° (θ_d), 46.0° (θ_e), and 124.5° (θ_f), respectively (see Fig. S3 in ESI† for details). Considering the dihedral angle in **4T** (54.3°), determined using X-ray crystallography,[4e] the smallest dihedral angle in **4T**, **5T**, and **6T** decreases with increasing number of thiophene rings.

In order to gain insight into the size-dependent structural characteristics, DFT calculations were conducted. The structures of **5T** and **6T**, optimized at the B3LYP-D3/6-31G(d) level nicely reproduced the structures observed by X-ray

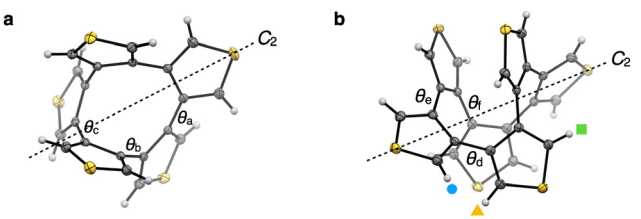

Fig. 3 (a) and (b) Molecular structures of **5T** (a) and **6T** (b) with thermal ellipsoids at 50% probability; gray = carbon; yellow = sulfur; white = hydrogen. The C_2 axis of **5T** and one of the C_2 axes of **6T** are noted with dashed lines. The hydrogen atoms indicated by the colored marks correspond to the ^{1}H NMR signals shown in Fig. 2b.

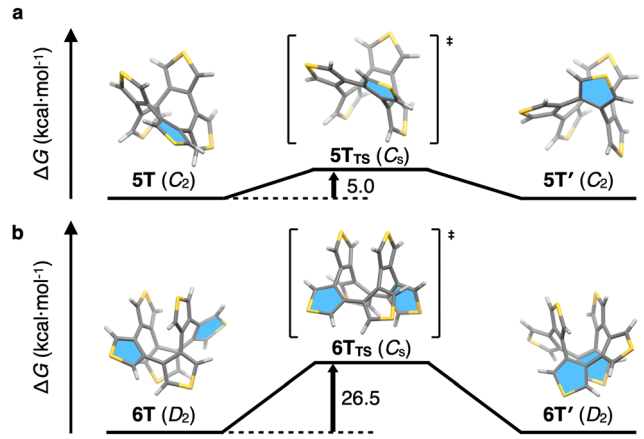

Fig. 4 Energy diagrams for the enantiomerization of **5T** (a) and **6T** (b). Selected thiophene rings are highlighted in blue to illustrate the enantiomerization.

crystallography, including the dihedral angles (see Fig. S3 in ESI† for details). Compound **6T** has two possible stable conformations, *i.e.*, a screw and a crown conformation.‡ The Gibbs free energy of **6T** with the screw conformation is 3.5 kcal mol^{-1} lower than that of the crown conformation, which was not observed by NMR spectroscopy in this study (see Fig. S4 in ESI† for details). Strain energies of **5T** and **6T** were calculated to be 19.9 and 1.1 kcal mol^{-1}, respectively, using hypothetical homodesmotic reactions.[15] This result indicates that **5T** has a strained structure, and the decrease in energy of **6T** might be due to the stabilization by intramolecular π–π interaction (see Fig. S5 in ESI† for details). The enantiomerization between C_2-symmetric **5T** and **5T′** as well as between D_2-symmetric **6T** and **6T′** is illustrated in Fig. 4a and b. Our calculations suggest C_s symmetry for the transition states (TSs) of **5T** and **6T**, and activation energies for the interconversion of **5T** and **6T** of 5.0 and 26.5 kcal mol^{-1}, respectively. The highlighted thiophene ring resides initially on the C_2 axis in **5T**; after interconversion *via* the enantiomerization pathway, this thiophene ring does not reside anymore on the C_2 axis in **5T′**. By repeating these enantiomerization steps, all α-protons become magnetically equivalent. This dynamic motion, together with the low activation energy, leads to a rapid exchange of the α-protons even at low temperatures. In the enantiomerization process of **6T**, the highlighted thiophene rings on the C_2 axis become the central thiophene rings, and four thiophene rings are symmetrically identical. Although this process leads to the magnetic equivalence of the α-protons, the reaction rate should be slow because of the high activation energy (26.5 kcal mol^{-1}). Taken together, the NMR spectrum of **4T** shows a singlet because of its highly symmetric structure (D_{2d}). Although **5T** has low symmetry (C_2), the fast dynamic motion of the molecule enables the α-protons of the thiophene rings to reach magnetic equivalence. Compound **6T** also has low symmetry (D_2), albeit that its unsymmetrical NMR signals indicate a slow exchange of the diastereotopic α-protons on the NMR timescale. Thus, the size-dependent structural characteristics of **4T**, **5T**, and **6T** were determined using a combination of NMR measurements and DFT calculations.

To further examine the size-dependent characteristics of **5T**, **6T**, and reference compound **4T**, their UV-vis absorption spectra were recorded (Fig. 5a). The maximum absorption for all three compounds was observed at ∼230 nm, and the longest-wavelength absorption maxima were observed at 263, 273, and 276 nm for **4T**, **5T**, and **6T**, respectively. Fluorescence of **5T** and **6T** was negligible in dichloromethane solution. The frontier molecular orbitals related to the longest absorption bands and their energy levels are depicted in Fig. 5b, taking into account the vertical excitation energies, oscillator strengths, and transition contributions obtained from time-dependent (TD) DFT calculations (see Fig. S6 in ESI† for details). Because **4T** adopts a highly symmetrical structure, the electronic wavefunctions of the HOMO and LUMO are distributed over the entire molecule, and the HOMO and the HOMO−1 are degenerate. In contrast, the HOMO and LUMO of **5T** and **6T** are relatively localized, presumably because of their lower-symmetry structures. The shoulder peaks in the range of 260–280 nm can be attributed to a combination of the HOMO−1 → LUMO and HOMO → LUMO transitions for **4T**, and the HOMO → LUMO transitions for **5T** and **6T**. With increasing number of thiophene rings, the HOMO level rises gradually from −6.09 eV to −5.76 eV, while the LUMO energy decreases from **4T** to **5T** and is similar for **5T** and **6T**. Consequently, it can be concluded that the HOMO–LUMO energy gap decreases from **4T** to **6T**, which is consistent with the bathochromic shift observed for the longest-wavelength absorption maxima.

In summary, we have developed synthetic routes to **5T** and **6T** *via* Suzuki–Miyaura cross-coupling and a Ni-mediated

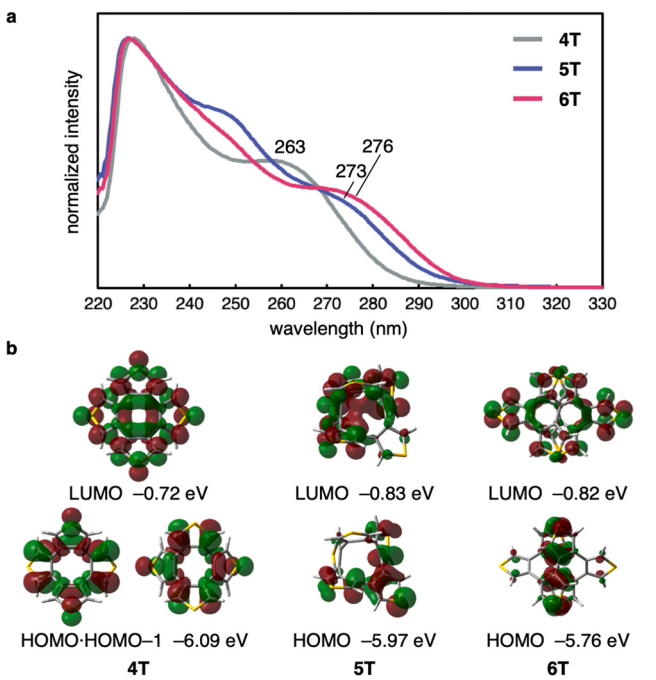

Fig. 5 Optoelectronic properties of **4T**, **5T**, and **6T**. (a) UV-vis absorption spectra of **4T**, **5T**, and **6T** in CH_2Cl_2. (b) Frontier molecular orbitals and the energy levels of **4T**, **5T**, and **6T** calculated at the B3LYP-D3/6-31G(d) level (isovalue = 0.03).

homocoupling reaction that involved the synthesis of a new β,β′-substituted moiety **2**. Using an excess of **3** effectively suppressed the formation of polymers. While only a single singlet was observed in the NMR spectra of **4T** and **5T**, three different signals were observed for **6T**. The solid-state structures of **5T** and **6T** were determined using X-ray crystallography; a corresponding analysis of the metric parameters revealed that the smallest dihedral angle of the 3,3′-bithiophene moiety decreases with increasing number of thiophene rings. The size-dependence observed in the NMR spectra can be rationally interpreted in terms of the activation energies for the interconversion of the thiophene rings. The size-dependence manifests in the optoelectronic measurements, in which the longest-wavelength absorption maxima are by 13 nm bathochromically shifted with increasing size of the molecules. The results of our DFT calculations suggest that gradually increasing the number of thiophene rings gradually increases the HOMO energy and decreases the LUMO energy. With synthetic routes to **5T** and **6T** established, it will now be possible to explore the synthetic chemistry of a variety of unprecedented thiophene-containing arenes.

This work was supported by FOREST program (JPMJFR211R to Y. S.) from JST, JSPS KAKENHI (JP22K19038 and JP22H02068 to Y. S.), UBE Foundation, Mitsubishi Foundation, and Asahi Glass Foundation. We thank Tetsuro Kusamoto, Ryota Matsuoka (IMS) and Takayuki Tanaka (Kyoto Univ.) for their support of experiments and fruitful advices. M. N. is a recipient of JSPS Research Fellowship for Young Scientists (DC2) and IMS SRA fellowship. This work was conducted in IMS supported by ARIM (JPMXP1223MS5012). Calculations were performed using the resources of the Research Center for Computational Science, Okazaki, Japan (23-IMS-C202).

Conflicts of interest

There are no conflicts to declare.

Notes and references

‡ Crown conformer is observed in hexaphenylene[2b,e–g] and hexa(2,3-thienylene)s.[4a,11a]

1 (*a*) A. Mishra, C.-Q. Ma and P. Bäuerle, *Chem. Rev.*, 2009, **109**, 1141; (*b*) M. Iyoda, J. Yamakawa and M. J. Rahman, *Angew. Chem., Int. Ed.*, 2011, **50**, 10522; (*c*) M. Stępień, N. Sprutta and L. Latos-Grażyński, *Angew. Chem., Int. Ed.*, 2011, **50**, 4288; (*d*) J.-i Setsune, *Chem. Rev.*, 2017, **117**, 3044; (*e*) M. Hermann, D. Wassy and B. Esser, *Angew. Chem., Int. Ed.*, 2021, **60**, 15743.

2 (*a*) W. C. Lothrop, *J. Am. Chem. Soc.*, 1941, **63**, 1187; (*b*) G. Wittig and G. Lehmann, *Liebigs Ann. Chem.*, 1957, **90**, 875; (*c*) G. Wittig and F. Bickelhaupt, *Chem. Ber.*, 1958, **91**, 883; (*d*) C. M. Buess and D. D. Lawson, *Chem. Rev.*, 1960, **60**, 313; (*e*) G. Wittig and K.-D. Rümpler, *Liebigs Ann. Chem.*, 1971, **751**, 1; (*f*) H. Irngartinger, *Isr. J. Chem.*, 1972, **10**, 635; (*g*) L. Ernst, A. Mannschreck and K.-D. Rümpler, *Org. Magn. Reson.*, 1973, **5**, 125; (*h*) H. Irngartinger, *Acta Crystallogr.*, 1973, **B29**, 894; (*i*) H. J. S. Winkler and G. Wittig, *J. Org. Chem.*, 1963, **28**, 1733; (*j*) J.-W. Han, X.-S. Peng and H. N. C. Wong, *Natl. Sci. Rev.*, 2017, **4**, 892; (*k*) D. Sonet and B. Bibal, *Tetrahedron Lett.*, 2019, **60**, 872; (*l*) H. Takano, T. Ito, K. S. Kanyiva and T. Shibata, *Eur. J. Org. Chem.*, 2019, 2871; (*m*) N. Contreras-Pereda, S. Pané, J. Puigmartí-Luis and D. Ruiz-Molina, *Coord. Chem. Rev.*, 2022, **460**, 214459; (*n*) H.-R. Ma, X.-S. Peng, J.-F. Cui and H. N. C. Wong, *Tetrahedron Lett.*, 2023, **119**, 154429.

3 (*a*) K. Takimiya, S. Shinamura, I. Osaka and E. Miyazaki, *Adv. Mater.*, 2011, 4347; (*b*) Y. Lin, Y. Li and X. Zhan, *Chem. Soc. Rev.*, 2012, **41**, 4245; (*c*) T. Okamoto, C. P. Yu, C. Mitsui, M. Yamagishi, H. Ishii and J. Takeya, *J. Am. Chem. Soc.*, 2020, **142**, 9083; (*d*) Q. Shen, C. He, S. Li, L. Zuo, M. Shi and H. Chen, *Acc. Mater. Res.*, 2022, **3**, 644.

4 (*a*) T. Kauffmann, B. Greving, J. König, A. Mitschker and A. Woltermann, *Angew. Chem., Int. Ed. Engl.*, 1975, **14**, 713; (*b*) H. Hart and M. Sasaoka, *J. Am. Chem. Soc.*, 1978, **100**, 4326; (*c*) H. Irngartinger, U. Huber-Patz and H. Rodewald, *Acta Crystallogr.*, 1985, **C41**, 1088; (*d*) M. K. Shepherd, *J. Chem. Soc., Chem. Commun.*, 1985, 880; (*e*) T. Fujimoto, R. Suizu, H. Yoshikawa and K. Awaga, *Chem. – Eur. J.*, 2008, **14**, 6053.

5 K. Imamura, K. Takimiya, Y. Aso and T. Otsubo, *Chem. Commun.*, 1999, 1859.

6 (*a*) K. Y. Chernichenko, V. V. Sumerin, R. V. Shpanchenko, E. S. Balenkova and V. G. Nenajdenko, *Angew. Chem., Int. Ed.*, 2006, **45**, 7367; (*b*) A. Dadvand, F. Cicoira, K. Y. Chernichenko, E. S. Balenkova, R. M. Osuna, F. Rosei, V. G. Nenajdenko and D. F. Perepichka, *Chem. Commun.*, 2008, 5354; (*c*) S. Kato, Y. Serizawa, D. Sakamaki, S. Seki, Y. Miyake and H. Shinokubo, *Chem. Commun.*, 2015, **51**, 16944; (*d*) Y. Serizawa, S. Akahori, S. Kato, H. Sakai, T. Hasobe, Y. Miyake and H. Shinokubo, *Chem. – Eur. J.*, 2017, **23**, 6948; (*e*) S. Akahori, H. Sakai, T. Hasobe, H. Shinokubo and Y. Miyake, *Org. Lett.*, 2018, **20**, 304; (*f*) L. Li, S. Zhao, B. Li, L. Xu, C. Li, J. Shi and H. Wang, *Org. Lett.*, 2018, **20**, 2181; (*g*) S. Kato, S. Akahori, Y. Serizawa, X. Lin, M. Yamauchi, S. Yagai, T. Sakurai, W. Matsuda, S. Seki, H. Shinokubo and Y. Miyake, *J. Org. Chem.*, 2020, **85**, 62; (*h*) Y. Miyake and H. Shinokubo, *Chem. Commun.*, 2020, **56**, 15605; (*i*) S. Akahori, T. Sasamori, H. Shinokubo and Y. Miyake, *Chem. – Eur. J.*, 2021, **27**, 8178; (*j*) S. Akahori, T. Fujihara, Y. Tsuji, H. Shinokubo and Y. Miyake, *Synthesis*, 2021, 2995.

7 (*a*) S. Zhang, X. Liu, C. Li, L. Li, J. Song, J. Shi, M. Morton, S. Rajca, A. Rajca and H. Wang, *J. Am. Chem. Soc.*, 2016, **138**, 10002; (*b*) C. Zhao, X. Cai, Z. Ma, J. Shi, L. Xu and H. Wang, *J. Photochem. Photobiol., A*, 2018, **355**, 318; (*c*) A. Rajca, C. Shu, H. Zhang, S. Zhang, H. Wang and S. Rajca, *Photochem. Photobiol.*, 2021, **97**, 1376.

8 T. Takeda, M. Ozawa and T. Akutagawa, *Cryst. Growth Des.*, 2019, **19**, 4784.

9 T. Sugano, T. Hashida, A. Kobayashi, H. Kobayashi and M. Kinoshita, *Bull. Chem. Soc. Jpn.*, 1988, **61**, 2303.

10 A. Patra, Y. H. Wijsboom, L. J. W. Shimon and M. Bendikov, *Angew. Chem., Int. Ed.*, 2007, **46**, 8814.

11 Examples of cyclic structures including β,β′-linkages: (*a*) M. J. Marsella, K. Yoon and F. S. Tham, *Org. Lett.*, 2001, **3**, 2129; (*b*) Y. Wang, Z. Wang, D. Zhao, Z. Wang, Y. Cheng and H. Wang, *Synlett*, 2007, 2390; (*c*) F. Sannicolò, P. R. Mussini, T. Benincori, R. Cirilli, S. Abbate, S. Arnaboldi, S. Casolo, E. Castiglioni, G. Longhi, R. Martinazzo, M. Panigati, M. Pappini, E. Q. Procopio and S. Rizzo, *Chem. – Eur. J.*, 2014, **20**, 15298; (*d*) K. Asai, A. Fukazawa and S. Yamaguchi, *Chem. Commun.*, 2015, **51**, 6096; (*e*) C. Zhao, L. Xu, Y. Wang, C. Li and H. Wang, *Chin. J. Chem.*, 2015, **33**, 71; (*f*) M. Ueda, K. Jorner, Y. M. Sung, T. Mori, Q. Xiao, D. Kim, H. Ottosson, T. Aida and Y. Itoh, *Nat. Commun.*, 2017, **8**, 346; (*g*) E. Quartapelle Procopio, T. Benincori, G. Appoloni, P. R. Mussini, S. Arnaboldi, C. Carbonera, R. Cirilli, A. Cominetti, L. Longo, R. Martinazzo, M. Panigati and R. Pò, *New J. Chem.*, 2017, **41**, 10009.

12 K. Kise, F. Chen, K. Kato, T. Tanaka and A. Osuka, *Chem. Lett.*, 2017, **46**, 1319.

13 A. Rajca, M. Miyasaka, M. Pink, H. Wang and S. Rajca, *J. Am. Chem. Soc.*, 2004, **126**, 15211.

14 P. Leowanawat, A.-M. Resmerita, C. Moldoveanu, C. Liu, N. Zhang, D. A. Wilson, L. M. Hoang, B. M. Rosen and V. Percec, *J. Org. Chem.*, 2010, **75**, 7822.

15 V. I. Minkin, *Pure Appl. Chem.*, 1999, **71**, 1919.

